Crimson Publishers
Wings to the Research

Mini Review

Path Planning of Spatial Mechanisms Using Artificial Intelligence

Ilias Chouridis[1], Gabriel Mansour[2]*, Vasileios Papageorgiou[2], Michel Theodor Mansour[2] and Apostolos Tsagaris[1]

[1]Department of Industrial Engineering and Management, International Hellenic University, Greece

[2]Department of Mechanical Engineering, Aristotle University of Thessaloniki, Greece

ISSN: 2832-4463

***Corresponding author:** Gabriel Mansour, Department of Mechanical Engineering, Aristotle University of Thessaloniki, Greece

Submission: September 18, 2025
Published: November 04, 2025

Volume 5- Issue 1

How to cite this article: Ilias Chouridis, Gabriel Mansour*, Vasileios Papageorgiou, Michel Theodor Mansour and Apostolos Tsagaris. Path Planning of Spatial Mechanisms Using Artificial Intelligence. COJ Rob Artificial Intel. 5(1). COJRA. 000603. 2025.
DOI: 10.31031/COJRA.2025.05.000603

Abstract

Mechanisms are crucial for the accomplishment of manufacturing and industrial procedures. An important factor for their operation is the integration of path planning algorithms to optimize the trajectory of the end effector. The path planning algorithms ensure that the mechanism's trajectory avoids the obstacles and simultaneously minimizes its length. The effectiveness of the artificial fish swarm algorithm in 3D path planning cases is examined. The generated paths are designed to be applied to spatial mechanisms. Their effective implementation is examined by the execution of the resulting path using an industrial robotic arm in real-world scenario.

Keywords: Artificial intelligence; Path planning; Mechanisms; Spatial mechanisms; Artificial fish swarm algorithm; Industrial robotic arm; 3D path planning

Introduction

Mechanical mechanisms are the foundation of modern machinery providing the framework through which theoretical principles of mechanics are transformed into practical applications. The advancements of industrial development led to the establishment of more sophisticated systems of mechanisms that enable the precise conversion of input energy into predefined and controlled motions. Spatial mechanisms are a main category of mechanical systems. In spatial mechanisms the motion of one or more of their bodies is performed in different planes [1,2]. As a result, the movement of their end effectors is executed in 3D. Kinematic analysis predicts the response of the mechanism to a given input motion [3] based on the position, velocity, and acceleration of its components. The Degrees of Freedom (DoF) of a mechanism are defined as the number of independent movements it can execute [4]. The workspace of a mechanism is a specific area that its end effector can operate in [5]. There are several algorithms that enable robots to move from a starting to an ending location. The path planning must be consistent with the robot's movement capabilities. Thus, the path planning process of spatial mechanisms requires a 3D trajectory generation. There are several algorithms that solve the path planning problem in 3D [6-9] and 4D [10-12].

Researchers have proposed several algorithms to solve the 3D path planning problem. Yang et al. [13] implemented a Particle Swarm Algorithm (PSO) for solving the path planning of flexible needle navigation through an environment with several obstacles in the context of percutaneous puncture surgery [13]. Li et al. [14] presented an A* for solving the 3D path planning algorithm problem in nuclear emergency situations [14]. Niu et al. [15] proposed a continuous Ant Colony Optimization (ACO) algorithm for generating the 3D course of unmanned aerial vehicles in an environment with static obstacles [15]. Song et al. [16] nominated a reinforcement learning fast dual Rapid Exploring Tree (RRT) for addressing the 2D and 3D path planning of unmanned underwater vehicles [16].

In this paper the application of a 3D [17] path planning algorithm is examined for spatial mechanisms. The resulting path avoids collisions with the obstacles in the mechanism's working environment and reflects the shortest connection between a starting and an ending point. The feasibility of the path is examined using a real-world 6 DoF industrial robotic arm. The path's simulation in an industrial robotic arm with advanced configuration verifies that it can also be applied to spatial mechanisms with simpler kinematics.

Methodology

The virtual modeling of the real-world environment was achieved using the grid method. The grid method divides space into individual elementary units with specific dimensions. At the center of gravity of each elementary unit, a discrete point is placed, which represents the space occupied by the elementary unit. Obstacles encountered in the real world are defined in the grid environment by prohibiting movement towards the corresponding discrete points. Each discrete point is assigned with the numerical value 1 if it is not an obstacle and with the value 0 when it is considered as an obstacle. The Artificial Fish Swarm Algorithm (AFSA) is a bio-inspired algorithm that imitates 4 behaviors of real-world fish swarms. The bio-inspired algorithms are a category of artificial intelligence algorithms to solve optimization problems [18,19]. AFSA demonstrates a highly effective global search capability, enabling it to thoroughly explore the solution space and identify alternative feasible routes within the workspace [20]. Compared to other traditional bio-inspired optimization techniques, AFSA can also converge to the optimal solution in less time. Moreover, AFSA can lead to reliable results with low dependency on the value of initial parameters [21]. The generation of the path in AFSA is achieved by mimicking the prey, swarm, follow behavior and random behavior of the fish swarms in the real world. The behaviors utilized for the selection of the next possible movement point are based on the swarm location on the grid. The prey, swarm and follow behaviors were adopted as described in the traditional AFSA [22] while the random behavior was replaced by the one proposed in [23]. The approaches of simple and advanced 3D elimination, the heatmap, the integration of the ray casting algorithm and the multiple laser activation method presented in [17] were adopted. It is noted that the multiple laser activation method was also modified for 2D path generation. The objective function used was the same as [17].

Result

The described 3D path planning algorithm was applied to generate collision free trajectories for a 6 DoF industrial robotic arm. The experiments were conducted using the Kawasaki RS010N robotic arm. The metal component has a length of lm=350mm, a height of hm=400mm and a thickness of wm=60mm. The diameter of the central hole is dm1=280mm and while the diameter of the smaller hole is dm2=100mm. The rectangular obstacle has a length of lr=850mm, a height of hr=560mm and a thickness of wr=25mm. The algorithm's parameters are the following the maximum number of iterations MaxIt=90, the population size numFish=150, the try-number fishTryNum=15, the highest number of steps before a path is deemed to be unoptimal and is subsequently rejected MaxStepsNum=40 and the crowding factor δ=0.2. The heatmap created using the following parameters, obsHeatVal=150, heatIncrCoef=0.4, obsNearHeatVal=90, obsNearHeatVal2=40. The hetmap's navigation strategy is the following. The heatmap values, hv, were initially analyzed in relation to the average value mh and the distance df of the examined point from the fish's location. If hv<0.92×mh, for the objective function's value of points, where their df=2×da is multiplied by bh=1.35×da. The variable da represents the length of the elementary unit. If hv≤1.08×mh and hv≥0.92×mh for the points distanced df=$\sqrt{2}$×da or df=da, bh=1.25. If hv>1.08×mh and hv≤1.28×mh for the points where df=$\sqrt{5}$×da, bh=0.82. The ray casting algorithm does not contain customizable parameters.

Figure1a shows the experimental set up. Figure 1b-1f show the position of the robotic arm during the execution of the resulting path. Figure 1g shows the grid environment and the resulting path. In red are shown the discrete points, in black the obstacles, in blue the starting point, in green the ending point and in magenta the final path. The utilized grid environment consists of 1400 discrete points and it is considered as dense. Its dimensions are 700×1200×500mm. The size of each elementary unit is 50×60×100mm. In the grid environment 92 points are defined as obstacles. A dense environment was selected due to the complex geometry of its obstacles. The grid's density is determined to achieve an optimal balance between spatial resolution and computational efficiency. In the examined environment, the obstacles are primarily concentrated within a specific area, while a substantial portion of the workspace remains unoccupied. The grid dimensions were selected to ensure an accurate representation of the obstacle regions while minimizing the impact of obstacle overexpansion. A thin facilitates the representation of the obstacle free region enabling the algorithm to locate the optimal solution more quickly, however, the limited accuracy in the representation of the obstacles would distort the course of the resulting path, leading to an increase in path length.

A dense grid environment can simulate more accurately the shape curved obstacles compared to a thin environment. The detailed simulation of these types of obstacles is attributed to the fact that each discrete point represents a smaller area. However, the increase in the number of discrete points also increases the computational requirements. The algorithm's computational time was 33,85 seconds. The test was executed on a computer with a CPU Intel(R) Core(TM) i7-7500U 2.70GHz, the GPU model was a AMD Radeon R7M340 and with 6GB RAM capacity (Figure 1).

Figure1f shows the resulting from the ACO [24] algorithm in the same grid environment. The total length using ACO is 1701,2mm. The length of the resulting path from the presented AFSA is 1235,4mm 27,3% shorter. The maximum path length of AFSA's implementation is maxAFSA=2725.7mm, the average path length avgAFSA=1702.3mm, the maximum nodes of the generated paths maxNodesAFSA=51 and the average nodes number avgAFSA=12.7315. The path generated by the AFSA algorithm

consists of 4 nodes, whereas the corresponding path obtained using the ACO algorithm comprises 20 nodes. Figure 1g show the variation of path length across iterations during the execution of the AFSA algorithm. Zero-length paths correspond to those that were discarded either because they exceeded the allowable number of nodes or terminated in a dead-end.

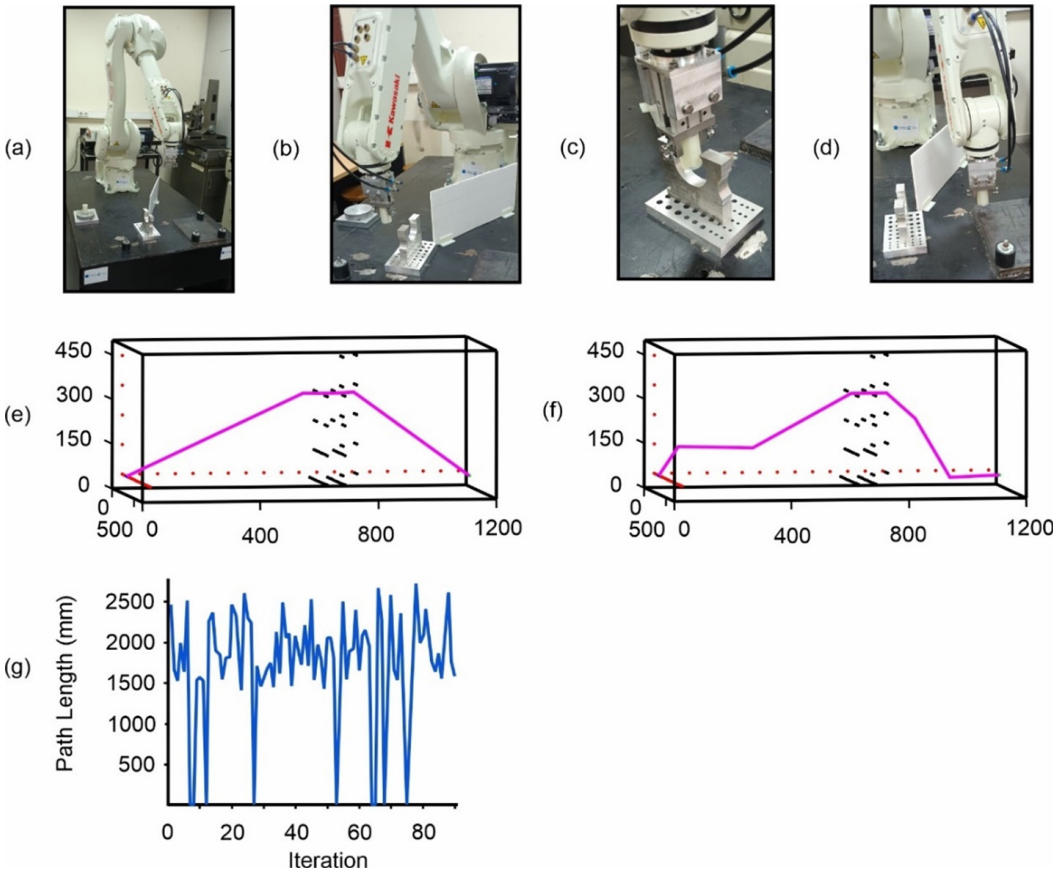

Figure 1: (a) Experimental set up, (b)-(d) Positions of the robot during path execution, (e) Resulting path utilizing AFSA, (f) Resulting path utilizing ACO [24] (g) Resulting diagram of path length per iteration for AFSA.

Discussion

The effective navigation of the end effector of spatial mechanisms is a crucial factor especially in the execution of advanced tasks. The application of AFSA in solving the path planning problem in 3D spaces proved to be particularly effective. The applications of path planning algorithms in mechanisms with complex kinematics such as industrial robotic arms verify that can also be applied to simpler mechanisms. Virtual representation of the real world is important for path generation. The dense grid environment can reduce discrepancies, potential collisions and oversized representation of obstacles between virtual and real world.

References

1. Barton M, Shragai N, Elber G (2025) Kinematic simulation of planar and spatial mechanisms using a polynomial constraints solver. Computer-Aided Design and Applications 6(1): 115-123.
2. Zhang Y, Finger S (2025) More on machines and mechanisms, Rapid Design through Virtual and Physical Prototyping. Carnegie Mellon University, USA.
3. Yu YQ, Zhou P, Xu QP (2019) Kinematic and dynamic analysis of compliant mechanisms considering both lateral and axial deformations of flexural beams. Proceedings of the Institution of Mechanical Engineers, Part C: Journal of Mechanical Engineering Science 233: 1007-1020.
4. Razmara N, Kohli D, Dhingra AK (2000) ON the degrees of freedom of motion of planar-spatial mechanisms. Proceedings of the ASME Design Engineering Technical Conferences and Computers and Information in Engineering Conference, USA, 7B: 1135-1141.
5. Merlet JP, Gosselin CM, Mouly N (1998) Workspaces of planar parallel manipulators. Mechanism and Machine Theory 33(1-2): 7-20.
6. Akay R, Yildirim MY (2025) SBA*: An efficient method for 3D path planning of unmanned vehicles. Mathematics and Computers in Simulation 231: 294-317.
7. Lei W, Wu X, Jia K, Han J (2025) UAV 3D path planning based on improved chimp optimization algorithm. Computers, Materials and Continua 83: 5679-5698.
8. Huang H, Song K, Chen Y, Jin H, Guan Y (2025) 3D path planning for AUVs under ocean currents by prioritized experience replay mechanism. Neurocomputing 630: 129719.
9. Hu G, Huang F, Shu B, Wei G (2025) MAHACO: Multi-algorithm hybrid ant colony optimizer for 3D path planning of a group of UAVs. Information Sciences 694: 121714.
10. Chouridis I, Mansour G, Papageorgiou V, Mansour MT, Tsagaris A (2025) Four-dimensional path planning methodology for collaborative robots' application in industry 5.0. Robotics 14(4): 48.

11. Tao B, Kim JH (2024) Mobile robot path planning based on bi-population particle swarm optimization with random perturbation strategy. Journal of King Saud University-Computer and Information Sciences 36: 101974.

12. Pollini L, Chouridis I, Mansour G, Chouridis A, Papageorgiou V, et al. (2025) Digital twin driven four-dimensional path planning of collaborative robots for assembly tasks in industry 5.0. Robotics 14(7): 97.

13. Yang T, Liu B, Sun R, Chen B, Ji G (2025) Path planning for flexible needle puncture based on multi-objective particle swarm optimization. Applied Soft Computing 184: 113838.

14. Li YC, Yang ZH, Tian H, Li ZY, Huo QC, et al. (2026) A three-dimensional space path planning method based on A* algorithm in radiation environment. Progress in Nuclear Energy 191: 106042.

15. Niu B, Wang Y, Liu J, Yue GXG (2025) Path planning for unmanned aerial vehicles in complex environment based on an improved continuous ant colony optimisation. Computers and Electrical Engineering 123: 110034.

16. Song Y, Chen G, Chen Y, Gao J (2025) Reinforcement learning-based fast-dual-tree RRT Path planning for unmanned underwater vehicles. Ocean Engineering 342: 122937.

17. Chouridis I, Mansour G, Papageorgiou V, Mansour MT, Tsagaris A (2025) Enhanced hybrid artificial fish swarm algorithm for three-dimensional path planning applied to robotic systems. Robotics 14(3): 32.

18. Poudel S, Arafat MY, Moh S (2023) Bio-inspired optimization-based path planning algorithms in unmanned aerial vehicles: A survey. Sensors 23(6): 3051.

19. Jakšić Z, Devi S, Jakšić O, Guha KA (2023) Comprehensive review of bio-inspired optimization algorithms including applications in microelectronics and nanophotonics. Biomimetics 8(3): 278.

20. Zainal N, Zain AM, Sharif S (2015) Overview of artificial fish swarm algorithm and its applications in industrial problems. Applied Mechanics and Materials 815: 253-257.

21. Pourpanah F, Wang R, Lim CP, Wang XZ, Yazdani D (2023) A review of artificial fish swarm algorithms: Recent advances and applications. Artificial Intelligence Review 56: 1867-1903.

22. Xll I, Shao ZJ, Qian JX (2002) An optimizing method based on autonomous animats: Fish-swarm algorithm. Systems Engineering-Theory & Practice 22: 32-38.

23. Chouridis I, Mansour G, Tsagaris A (2024) Three-dimensional path planning optimization for length reduction of optimal path applied to robotic systems. Robotics 13(12): 178.

24. Mansour G, Chouridis I, Tsagaris A (2024) Finding the optimal path in a 3D environment with predefined obstacles. International Journal of Advanced Mechatronic Systems 11(1): 50-62.